(17) Koningsveld, R.; Kleintjens, L. A.; Leblans-Vinck, A. M. *J. Phys. Chem.* **1987,** *91,* 6423.

(18) Gibbs, J. W. *Trans. Conn. Acad. Art. Sci.* **1874–78,** *3,* 108, 343.

(19) Modell, M.; Reid, R. C. *Thermodynamics and Its Applications*; Prentice Hall: Englewood Cliffs, NJ, 1971; Chapter 7.

(20) Morel, G.; Paul, D. R. *J. Membr. Sci.* **1982,** *10,* 273.

(21) Hillegers, L. T. M. E. Ph.D. Thesis, Technical University of Eindhoven, The Netherlands, 1986.

(22) Liau, I. S.; McHugh, M. A. In *Supercritical Fluid Technology*; Penninger, J. M. L., Radosz, M., McHugh, M. A., Krukonis, V. J., Eds.; Elsevier: New York, 1985.

(23) Beckman, E. J.; Porter, R. S.; Koningsveld, R. *J. Chem. Phys.* **1984,** *91,* 6429.

(24) Koningsveld, R. Ph.D. Thesis, University of Leiden, The Netherlands, 1967.

(25) Beckman, E. J.; Porter, R. S.; Koningsveld, R.; Kleintjens, L. A. In *Integration of Polymer Science and Technology*; Kleintjens, L. A., Lemstra, P. J., Eds.; Elsevier: New York, 1987; Vol. II.

(26) Lundberg, J. L.; Mooney, E. J.; Rogers, C. E. *J. Polym. Sci. A-2* **1969,** *7,* 947.

(27) Maloney, D. P.; Prausnitz, J. M. *Ind. Eng. Chem. Process Des. Dev.* **1976,** *15,* 216.

(28) Durrill, P. L.; Griskey, R. G. *AIChE J.* **1966,** *12,* 1147.

(29) Berens, A. R., personal communication.

(30) Bowman, L. M. Ph.D. Thesis, University of Utah, 1976.

(31) Sanchez, I. C.; Lohse, D. J. *Macromolecules* **1981,** *14,* 131.

(32) Koningsveld, R.; Stockmayer, W. H.; Kennedy, J. W.; Kleintjens, L. A. *Macromolecules* **1974,** *7,* 73.

(33) Irvine, P.; Gordon, M. *Macromolecules* **1980,** *13,* 761.

(34) Des Cloizeaux, J. *J. Phys. (Paris)* **1975,** *36,* 281.

(35) Edwards, S. F. *Proc. Phys. Soc., London* **1966,** *88,* 265.

(36) Muthukumar, M. *J. Chem. Phys.* **1986,** *85,* 4722.

(37) Beckman, E. J. Ph.D. Thesis, University of Massachusetts, 1988.

(38) Kumar, S. K.; Chhabria, S. P.; Reid, R. C.; Suter, U. W. *Macromolecules* **1987,** *20,* 2550.

(39) Smirnova, N. A.; Victorov, A. I. *Fluid Phase Equilib.* **1987,** *34,* 235.

(40) Bondi, A. *Physical Properties of Molecular Crystals, Liquids, and Glasses*; Wiley: New York, 1968.

Registry No. PMMA, 9011-14-7; PS, 9003-53-6; CO_2, 124-38-9.

Rheology of Ordered and Disordered Symmetric Poly(ethylenepropylene)–Poly(ethylethylene) Diblock Copolymers

J. H. Rosedale[†] **and F. S. Bates**[*,†]

AT&T Bell Laboratories, Murray Hill, New Jersey 07974. *Received August 24, 1989; Revised Manuscript Received November 6, 1989*

ABSTRACT: A series of poly(ethylenepropylene)–poly(ethylethylene) (PEP–PEE) diblock copolymers, containing 55% by volume PEP, and the corresponding PEP and PEE homopolymers have been investigated by dynamic mechanical spectroscopy. The ordered and disordered states are characterized by qualitatively different low-frequency rheological properties in close agreement with previous reports on this subject. This paper addresses three aspects of such behavior in the vicinity of the order–disorder transition: identification of the microphase-separation transition temperature, T_{MST}, evaluation of fluctuation effects, and characterization of the ordering kinetics. We identify T_{MST} based on the distinct discontinuity in G' ($\omega \ll \omega_c'$) and G'' ($\omega \ll \omega_c''$) that accompanies the order–disorder transition; $\omega_c' \cong 3\omega_c'' \ll \tau_d^{-1}$ delineates the beginning of the phase-state-dependent low-frequency regime where τ_d is the conventional single-chain longest relaxation time. Above and below T_{MST} the rheological properties are complex for $\omega < \omega_c$ (e.g., failure of time–temperature superposition), owing to the presence of composition fluctuations. In the disordered state these effects are evident 50 °C beyond T_{MST}. The magnitude of these fluctuation effects is underpredicted by recent theory, although the relative fluctuation contributions to the dynamic elastic and loss moduli are in quantitative agreement with theory. Quenching experiments from slightly above to just below T_{MST} reveal a ca. 10 °C region within which the ordering process can be followed rheologically. On the basis of the temporal evolution of G' ($\omega \ll \omega_c'$) following such temperature quenches, we conclude that the ordering process is governed by heterogeneous (secondary) nucleation.

I. Introduction

Block copolymer rheology has been shown in the past to be strongly dependent on morphology, which can be divided into two general categories. The ordered, or microphase-separated, state refers to the familiar periodically arranged spherical, cylindrical, lamellar, or bicontinuous double-diamond structures,[1] while the disordered state is spatially homogeneous. These two thermodynamic regimes are separated by the order–disorder transition (ODT), also referred to as the microphase separation transition (MST); here we use these expressions interchangeably. In all known block copolymers the segment–segment interaction parameter, χ, is linear with inverse temperature, thus producing a disordered material at sufficiently high temperatures. This situation is analogous to UCST behavior in binary polymer mixtures. Below the MST temperature (T_{MST}) block copolymers exist in the ordered state. We presently describe a detailed study of the dynamic mechanical properties of a nearly symmetric ($f = 0.55$) set of model poly(ethylenepropylene)–poly(ethylethylene) diblock copolymers, denoted PEP–PEE, both above and below T_{MST} where f corresponds to the volume fraction of the PEP block.

Nearly all previous investigations aimed at elucidating the relationships between rheology and morphology for block copolymers have relied upon materials composed of polystyrene and/or polydiene blocks, includ-

---

[†] Present address: Department of Chemical Engineering and Materials Science, University of Minnesota, Minneapolis, MN 55455.

0024-9297/90/2223-2329$02.50/0

ing polystyrene–polybutadiene–polystyrene (SBS)[2–4] and polystyrene–polyisoprene–polystyrene (SIS)[5–7] triblock copolymers and 1,4-polybutadiene-*cis*-1,4-polyisoprene[8] and 1,4-polybutadiene–1,2-polybutadiene (1,4-PB–1,2-PB)[9,10] diblock copolymers. All these studies have concluded that the MST is accompanied by gross changes in the rheological properties at low frequencies, although the precise establishment of T_{MST} and the detailed interpretation of the mechanical behavior around the transition remains somewhat controversial.[6]

Although the commercially important SBS and SIS thermoplastic elastomers have received much attention, these are not ideal materials for fundamental investigations of the rheology of block copolymers near the order–disorder transition. In order for T_{MST} to exist at a tractable temperature ($T \lesssim 200$ °C), these materials must be limited to rather low polystyrene block molecular weights, e.g., for $f = 1/2$, $M_{\mathrm{PS}} \lesssim 10^4$ g/mol. This precludes quantitative evaluation of statistical thermodynamic theories developed for high molecular weight polymers[11,12] and limits rheological studies to the disentangled state of this block.[13] Moreover, the relatively high value of T_g for polystyrene ($\sim$100 °C) further constrains T_{MST} since the MST must be well above T_g in order to observe this transition rheologically yet sufficiently low to allow testing of the disordered state without degradation. Preparation of 1,4-PB–1,2-PB diblock copolymers near the MST by Bates and co-workers[14] was motivated by the shortcomings of the polystyrene-based block copolymers. These materials are characterized by a variety of useful properties including a low T_g (<0 °C) and a moderate T_{MST} at a molecular weight well into the entangled regime for each block;[13] for example a $f = 0.38$, $M_w = 75\,400$ g/mol polymer is characterized by $T_{\mathrm{MST}} = 108$ °C. The order–disorder transition, determined from the discontinuity in isochronal plots of the elastic modulus and dynamic viscosity versus temperature, was found to be coincident with the identification of two branches in the dynamic moduli below a critical reduced frequency, ω_c, i.e., $G' \sim \omega^2$ and $G'' \sim \omega$ for $T > T_{\mathrm{MST}}$ and $G' \sim G'' \sim \omega^{0.5}$ for $T < T_{\mathrm{MST}}$. Similar dynamic moduli scaling is found with the SBS and SIS materials.[2–5] In addition, an anomalous departure from typical terminal behavior was observed in the disordered state as much as 50 °C above the MST in the 1,4-PB–1,2-PB materials,[10] which had not been reported previously. Subsequent theoretical work attributes this behavior to fluctuation effects.[15]

All of the block copolymers discussed thus far contain polydiene blocks which can readily cross-link when exposed to oxygen, heat, or radiation. Although precautions are usually taken to prevent degradation, e.g., deep-freeze inert-atmosphere storage and nitrogen purging during experimentation, any unexplained results from such studies are nevertheless suspect. Therefore, we were motivated to develop more resilient materials with which to investigate order and disorder in the entangled state, with the immediate objective of corroborating our prior finding regarding the identification of the MST and fluctuation effects.[10]

Recently we reported on the successful development of PEP–PEE, a fully saturated hydrocarbon diblock copolymer that retains all the desirable characteristics of 1,4-PB–1,2-PB and, in addition, exhibits much greater stability toward degradation.[16] In this paper we describe the linear dynamic mechanical properties of four nearly symmetric ($f = 0.55$) PEP–PEE diblock copolymers and the corresponding PEP and PEE homopolymers. This work clearly demonstrates the influence of composition fluctuations on the rheological properties around the MST and confirms the first-order nature of this transition for nearly symmetric samples. In addition, dynamic shear measurements obtained following a temperature quench from just above to just below T_{MST} demonstrate the ability to supercool the disordered material and provide a measure of the subsequent ordering kinetics. These findings fully corroborate the earlier results obtained for 1,4-PB–1,2-PB diblock copolymers.[10]

Table I
Characterization Results

sample	$10^{-3}M_{\mathrm{N}}$[a]	$M_{\mathrm{W}}/M_{\mathrm{N}}$[b]	PEP,[c] wt %	C_1[d]	C_2[d]
PEP–PEE-1	$31._5$	1.05	53	6.6_8	$146._8$
PEP–PEE-2	$50._1$	1.07	56	7.9_8	$148._6$
PEP–PEE-3	81.2	1.05	53	8.1_3	$151._5$
PEP–PEE-4	106	1.07	54	8.0_1	$141._0$
PEP	86.1	1.07	100	6.4_8	$173._1$
PEE	172	1.03	0	8.7_3	$148._5$

[a] Determined by membrane osmometry. [b] Determined by size-exclusion chromatography. [c] Determined by ^{13}C NMR. [d] WLF parameters.

II. Experimental Section

The synthesis and characterization of the four PEP–PEE diblock copolymers and the corresponding PEP and PEE homopolymers discussed in this report are described elsewhere.[16] Characterization results for these materials are listed in Table I. The PEP block contains 5% randomly distributed isopropylethylene and 95% alternating ethylenepropylene units, while the PEE block consists of 98% ethylethylene repeat units. All of the materials in this work are atactic and lack a crystalline melt transition.

Dynamic elastic and loss shear moduli, G' and G'', were determined for each material with a Rheometrics System IV rheometer operated in the oscillatory mode ($0.01 \le \omega \le 100$ rad/s) using 50-mm-diameter cone-and-plate test fixtures. Sample temperature was controlled (±1 °C) between 5 and 300 °C with a thermally regulated nitrogen gas purge. This temperature range is well above the glass transition temperatures reported earlier for these materials.[16] The cone-to-plate gap was kept constant by adjusting the apparatus at each measurement temperature in order to account for instrument thermal expansion.

Three different types of dynamic mechanical tests were employed in characterizing the rheological properties of PEP–PEE: isochronal temperature scans, isothermal frequency scans, and isothermal/isochronal time scans. The first set of experiments involved measuring the elastic modulus of PEP–PEE-2 and PEP–PEE-3 at a constant frequency over a select range of temperatures while heating the sample near the microphase separation transition. PEP–PEE-2 was tested at 1.0 rad/s between 85 and 105 °C with 2% and 20% strain amplitudes. PEP–PEE-3 was tested at 10.0 rad/s between 275 and 300 °C with a 2% strain amplitude. Exposure to the later extreme temperatures was restricted to less than 4 h during these experiments. Size-exclusion chromatography (SEC) traces of PEP–PEE-3 obtained before and after such tests were indistinguishable, thus demonstrating that degradation had not occurred; for times greater than approximately 4 h at 300 °C, chain scission became evident in the SEC traces. The second set of experiments consisted of conventional isothermal frequency scans conducted at a variety of temperatures for all six samples listed in Table I. In the third set of experiments, the dynamic shear moduli were measured over time at a constant frequency after quenching PEP–PEE-2 from the disordered state (i.e., above T_{MST}) to the ordered state (i.e., below T_{MST}). Seven quenches were performed from 100 °C to a temperature between 89 and 95 °C after which G' and G'' were continuously monitored at $\omega = 0.30$ rad/s. In each case approximately 10 min was required for the temperature of the sample to equilibrate, within the temperature resolution of the instrument, at the target temperature. In the isothermal frequency scans and the quench experiments the

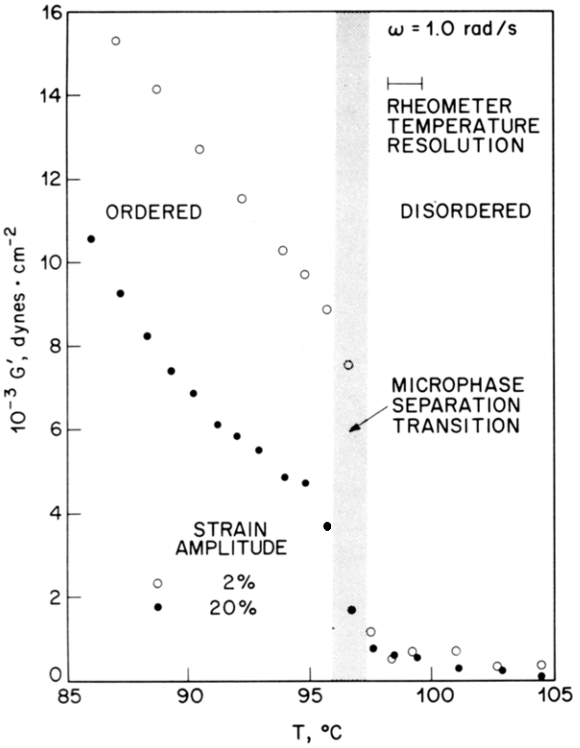

Figure 1. Temperature dependence of G' obtained at two strain amplitudes and a single frequency (ω = 1.0 rad/s) while heating sample PEP–PEE-2. The discontinuity in G' at 96 ± 1 °C results from the microphase separation transition.

maximum strain amplitude was kept at a constant low level (2–4%) so as to minimize nonlinear effects.

III. Results and Analysis

III.A. MST Temperatures. As with order–disorder transitions in low molecular weight systems, such as water, the microphase separation transition in block copolymers is accompanied by significant changes in various macroscopically observable physical properties. In the case of frozen and melted water these differences are immediately obvious. However, because the microphase separation transition is only weakly first order,[12] in contrast with the strong first-order character of the melting (freezing) transition in water, the corresponding property changes are more subtle. Nevertheless, these effects can be easily observed given sufficient time, as recently documented for the PEP–PEE block copolymers presently being discussed.[16] In order to precisely identify T_{MST}, we conducted low-frequency ($\omega < \omega_c$, see section III.B) isochronal dynamic shear measurements as a function of temperature on samples PEP–PEE-2 and PEP–PEE-3. Prior flow visualization and SAXS measurements[16] showed that T_{MST} = 91 ± 10 °C for PEP–PEE-2; similarly PEP–PEE-1 was shown to be disordered and PEP–PEE-3 and PEP–PEE-4 are ordered for $25 < T < 225$ °C. $G'(T)$ results for PEP–PEE-2 and PEP–PEE-3 are presented in Figures 1 and 2, respectively. In each case the elastic modulus decreases discontinuously (within the rheometer temperature resolution) at the MST. Using this technique, we have established T_{MST} = 96 ± 1 °C and 291 ± 1 °C for PEP–PEE-2 and PEP–PEE-3, respectively. In order to assess whether strain influences these measurements, we repeated the experiments on PEP–PEE-2 with 10 times the initial (2%) strain amplitude. As illustrated in Figure 1, below T_{MST} the apparent elastic modulus drops significantly with this increased strain amplitude, indicating a considerable nonlinear viscoelastic behavior; this effect will be further considered in the Discussion. However, our determination of T_{MST} as evidenced by the discontinuity in G' is unaffected by this increase in strain, leading us to conclude that the quoted MST temperatures are the true equilibrium (i.e., strain-free) values.

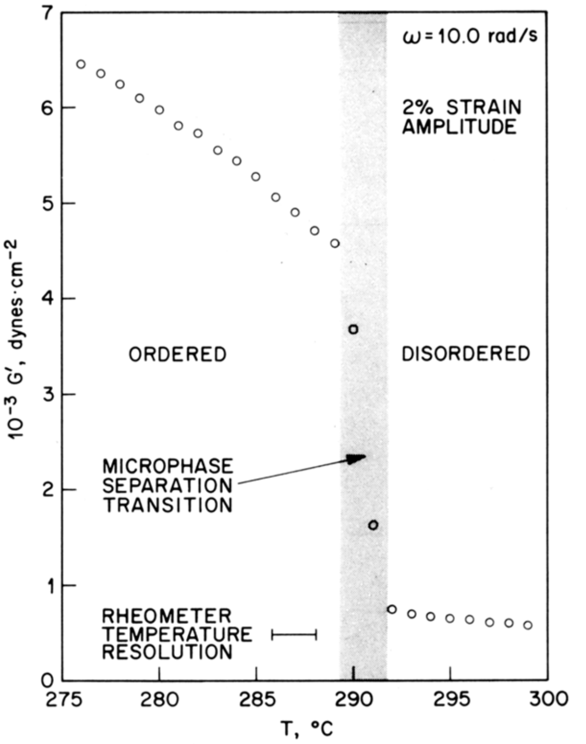

Figure 2. Temperature dependence of G' (ω = 10 rad/s) obtained while heating sample PEP–PEE-3. The sample disorders at 291 ± 1 °C.

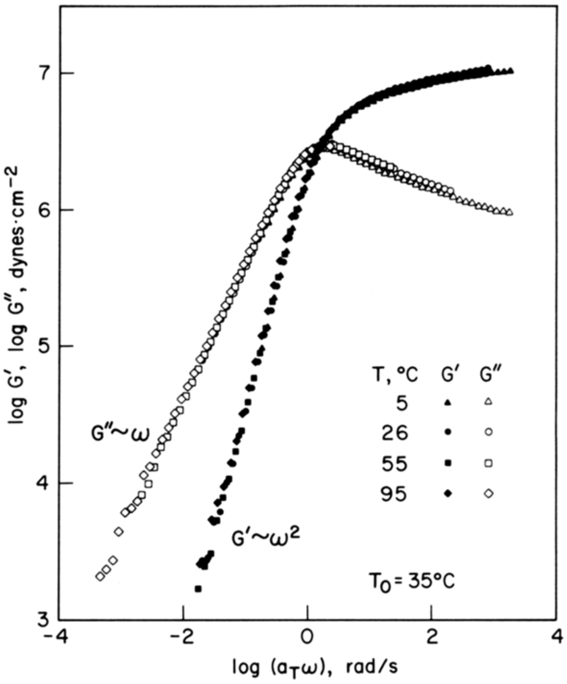

Figure 3. Master curves obtained from representative PEP homopolymer dynamic mechanical shear data.

III.B. Reduced Frequency Plots. The frequency-dependent viscoelastic properties for three of the four PEP–PEE diblock copolymers and the PEP and PEE homopolymers are illustrated in Figures 3–8. These reduced frequency plots were constructed using the time–temperature superposition principle[13] with a reference

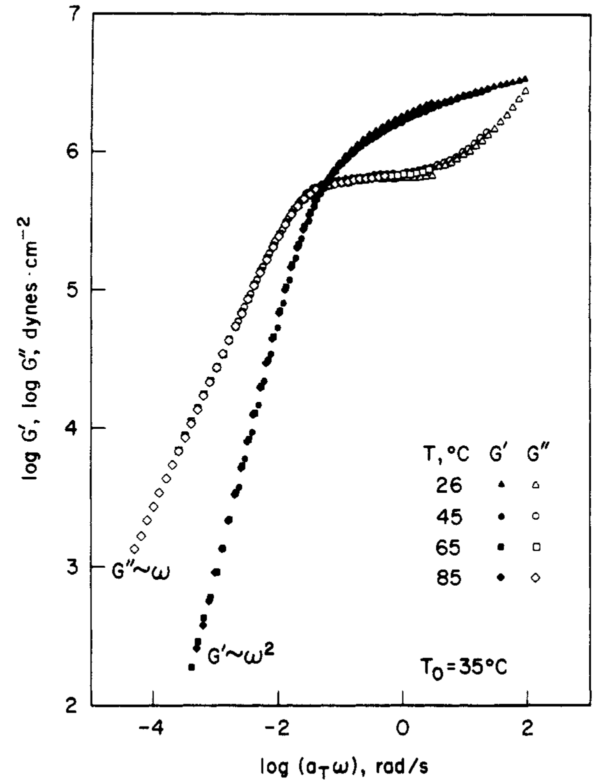

Figure 4. Master curves obtained from representative PEE homopolymer dynamic mechanical shear data.

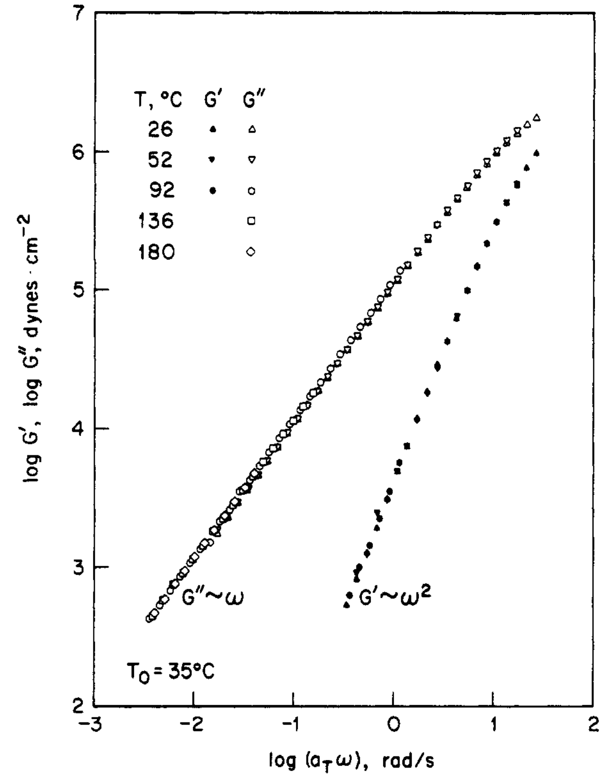

Figure 5. Master curves obtained from representative PEP–PEE-1 diblock copolymer dynamic mechanical shear data. Terminal relaxation behavior demonstrates that this material is disordered over the range of temperatures indicated.

temperature T_0 = 35 °C; vertical corrections of T_0/T were also applied to the data. Time–temperature superposition worked well for all values of frequency over the range of temperatures employed for PEP (Figure 3), PEE (Figure 4), PEP–PEE-1 (Figure 5), PEP–PEE-3 (not shown), and PEP–PEE-4 (Figure 6); the results for PEP–PEE-3 have been omitted since they are nearly identical in form with those for PEP–PEE-4. The results for PEP–PEE-2 are discussed below. In each case the shift factors a_T

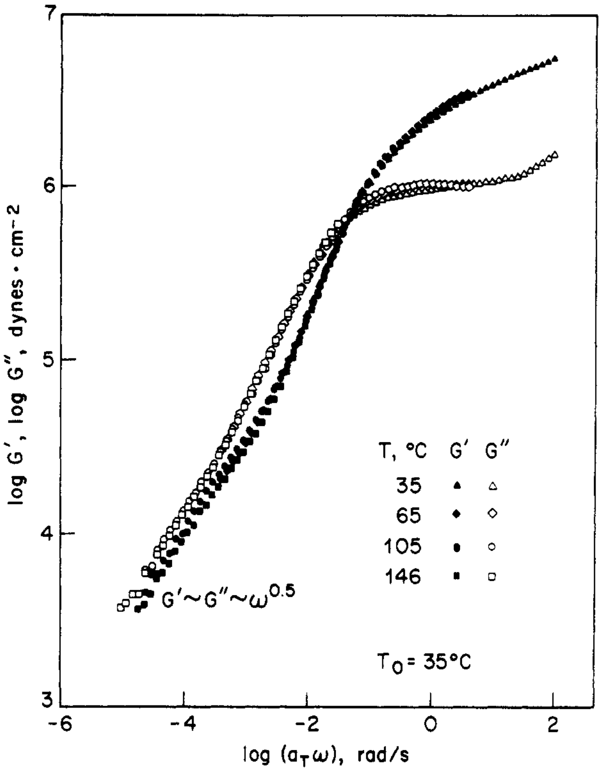

Figure 6. Master curves obtained from representative PEP–PEE-4 diblock copolymer dynamic mechanical shear data. The low-frequency power law behavior indicated is characteristic of the ordered state.

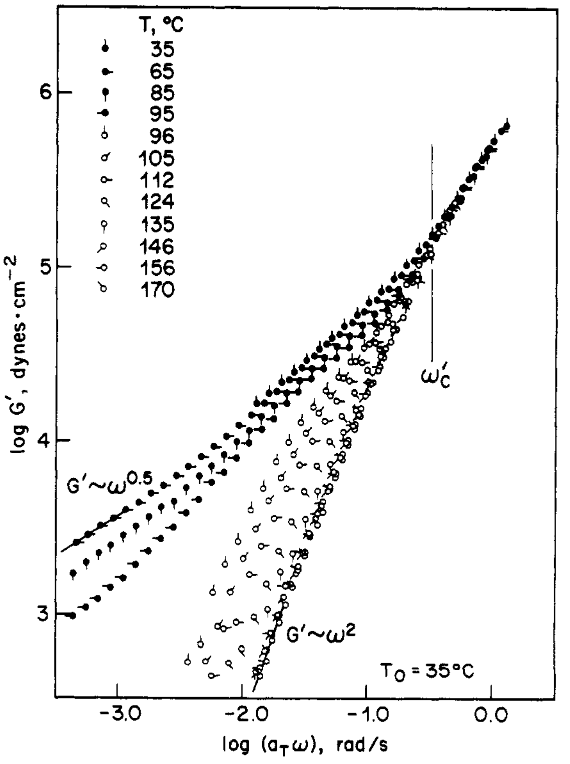

Figure 7. Reduced frequency plot for representative dynamic elastic data obtained from sample PEP–PEE-2. Shift factors were determined by concurrently superimposing G' and G'' data for $\omega > \omega'_c$ and $\omega > \omega''_c$ (see Figure 8), respectively. The filled and open symbols correspond to the ordered and disordered states. Failure of time–temperature superposition for $T \geq 96$ °C derives from fluctuation effects.

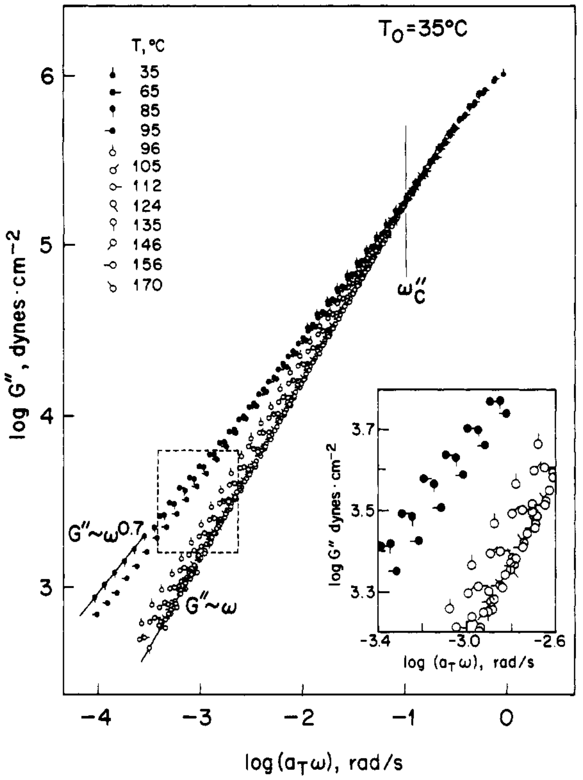

Figure 8. Reduced-frequency plot for representative dynamic loss data obtained from sample PEP–PEE-2. Symbol notation and shift factors are specified in Figure 7.

could be closely approximated by the WLF equation[13]

$$\log a_T = \frac{-C_1(T - T_o)}{C_2 + T - T_o} \quad (1)$$

where the fitted constants C_1 and C_2 are given in Table I.

The reduced-frequency plots generated for the homopolymers (Figures 3 and 4) show typical terminal linear viscoelastic behavior, i.e., $G' \sim \omega^2$ and $G'' \sim \omega$ as $\omega \rightarrow 0$. Similar terminal behavior is displayed by PEP–PEE-1 (Figure 5), which is consistent with the homogeneous nature of this sample.[16] In contrast, sample PEP–PEE-4, which is ordered over the entire temperature range investigated,[16] is characterized by nearly equivalent dynamic elastic and loss moduli at low reduced frequencies, $\log \omega_c' \lesssim -3.5$ and $\log \omega_c'' \lesssim -3$ (Figure 6), which scale as $G' \sim G'' \sim \omega^{0.5}$; ω_c' and ω_c'' are the values of $a_T\omega$ below which the effects of order and disorder are manifested. Thus, microphase separation dramatically influences the low-frequency rheological properties of PEP–PEE diblock copolymers, as seen previously with the 1,4-PB–1,2-PB materials.[10]

Unlike the low-frequency time–temperature superimposability of the dynamic shear moduli shown in Figures 3–6, the G' and G'' data for PEP–PEE-2, presented in Figures 7 and 8, do not superimpose below critical reduced frequencies of $\omega'_c \lesssim -0.5$ and $\omega''_c \lesssim -1.0$, respectively. These reduced frequency plots were constructed by superimposing the high-frequency branches ($\omega > \omega_c$) of the isothermal G' and G'' data; the corresponding WLF parameters are listed in Table I. For the highest measurement temperature (170 °C) the dynamic mechanical data do not extend beyond ω_c. Therefore, this set of low-frequency results was located in Figures 7 and 8 based on eq 1 using the WLF coefficients determined at lower temperatures. Here we note that although the use of time–temperature superposition on rheologically complex materials such as samples PEP–PEE-2 and PEP–PEE-4 is not rigorously correct, this method is useful in comparing the qualitative changes that occur at low frequencies near the MST. We comment further on this point in the Discussion.

As anticipated from our determination of T_{MST} (see Figure 1) the rheological behavior of PEP–PEE-2 (Figures 7 and 8) shows characteristics of both the ordered and disordered states as established by the results from samples PEP–PEE-4 (Figure 6) and PEP–PEE-1 (Figure 5), respectively. For example, at 35 °C PEP–PEE-2 behaves rheologically like PEP–PEE-4, e.g., $G'(\omega) \sim \omega^{0.5}$ for $\omega \ll \omega'_c$, while above 146 °C its behavior is essentially terminal as in the case of PEP–PEE-1. In addition, there is a lack of superimposability of the data between these temperatures below ω_c. Although this behavior is quite complex, a qualitative change is observed to occur at T_{MST}; i.e., for $T > 96$ °C, the low-frequency branch curves distinctly downward, whereas for $T < 96$ °C the curvature is decidedly upward. Also, as already indicated, for $T < T_{MST}$ and $\omega < \omega_c$, the results are highly strain-dependent (Figure 1), whereas for $T > T_{MST}$ we detected virtually no strain dependence in G' or G'' over the 0–20% range of strain amplitudes employed. This strain dependence derives from a tendency for the ordered block copolymer to orient in a shear field,[17] thus producing an anisotropic material with a commensurate reduction in G'. A detailed discussion of this effect is presented in a separate report.[18] Here we note that heating the sample above T_{MST} rapidly (less than a minute) erases any anisotropy imparted to the microphase-separated material, much like the effect obtained when melting single crystalline (i.e., "oriented") water. Subsequent cooling (i.e., "recrystallization") leads to a complete recovery of the original unsheared state.

These discontinuities in physical properties characterize the order–disorder transition. However, unlike strong first-order transitions, such as the melting or freezing of water where the physical properties immediately above and below the transition temperature remain essentially unaffected by the proximity to a phase transition, the weakly first-order MST is driven by fluctuations,[12] which become apparent at temperatures well above and below T_{MST}. A recent small-angle neutron scattering study of a partially deuterated PEP–PEE diblock copolymer clearly demonstrates the central role of fluctuations in inducing the weak first-order microphase separation transition.[19] The failure of time–temperature superposition above and below T_{MST} evident in Figure 7, and to a lesser extent in Figure 8, is a direct manifestation of these fluctuations, which respond to changes in temperature differently (i.e., as shown by Fredrickson and Helfand[15]) than do the classical viscoelastic responses. Because these fluctuation effects reflect a collective response from many polymer chains, they naturally appear at frequencies well below the single-chain terminal frequency, $\omega \approx \tau_d^{-1}$. However, the *continuous* development of this low-frequency rheological behavior is quite distinct from the *discontinuous* change in properties at 96 °C for PEP–PEE-2, which can be unambiguously attributed to the MST.

In contrast with the low-frequency behavior ($\omega < \omega_c$), the high-frequency ($\omega > \omega_c$) PEP–PEE-2 data show no evidence of the microphase separation transition as illustrated in the inset of Figure 9. However, the WLF equations determined for each block copolymer do vary systematically between those determined for the corresponding homopolymers as seen in Figure 9. In fact, there appears to be a jump in the location of the shift factor

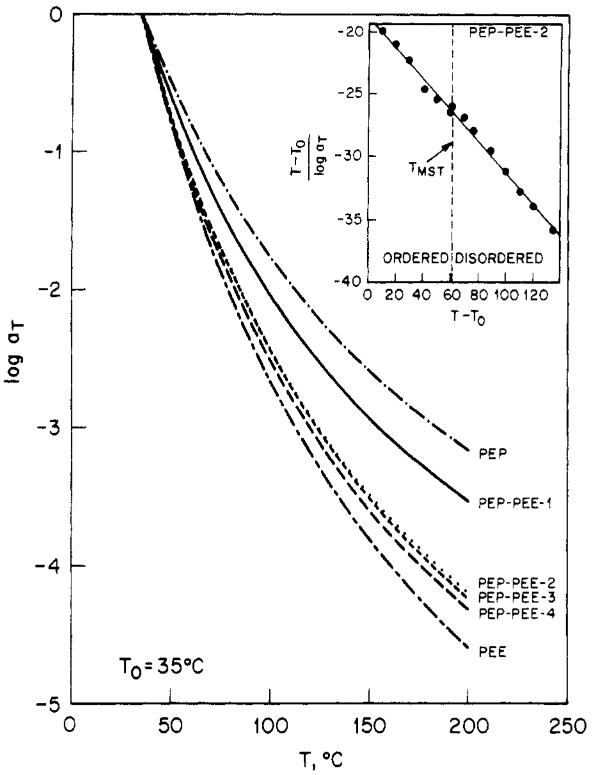

Figure 9. Comparison of the WLF shift factor curves for the six polymers studied in this work. The jump in location from PEP-PEE-1 to PEP-PEE-2, -3, and -4 is consistent with the presence of large composition fluctuations in sample PEP-PEE-2 just above T_{MST}. However, the MST does not noticeably influence the WLF parameters as shown in the inset.

curves in going from PEP-PEE-1, which lies close to that for PEP, to PEP-PEE-2, -3, and -4, which are grouped closely together near the result for PEE. A discussion of these findings is presented in section IV.B.

III.C. Quench Experiments. The rheological behavior of the PEP-PEE diblock copolymers clearly depends on phase state. During the course of our initial experimentation with PEP-PEE-2 we discovered that under certain conditions the ordered low-frequency response, i.e., $G' \sim G'' \sim \omega^{0.5}$, required a finite time to develop after the diblock copolymer had been quenched below T_{MST} from the disordered state. Where this time equaled or exceeded the time necessary to achieve thermal equilibration, we were able to monitor the evolution of the dynamic moduli as the ordered phase developed. Figure 10 depicts the growth of G' for PEP-PEE-2 at 92 °C ($\Delta T = T_{MST} - T = 4$ °C) following a quench from 100 °C ($\Delta T = -4$ °C). These measurements were taken at a constant frequency of 0.3 rad/s ($\log a_T\omega = -2.74$), which is well below the critical reduced frequency, ω_c.

For $\Delta T = 4$ °C the dynamic elastic shear modulus increases in magnitude for approximately 46 min following thermal equilibration (Figure 10). Anticipating that the ordering kinetics represent a crystallization process, we have modeled our time-dependent rheological results using the Avrami equation[20]

$$X(t) = 1 - \exp(-kt^n) \qquad (2)$$

which is conventionally used to relate the fractional crystallization, $X(t)$, to time t through a crystallization rate constant, k, where the exponent n may take on a value between 1 and 4 depending upon the dimensionality of crystal growth and the nature of the rate-limiting step. In general, $X(t)$ is obtained through a direct measurement of sample crystallinity, e.g., by monitoring density.

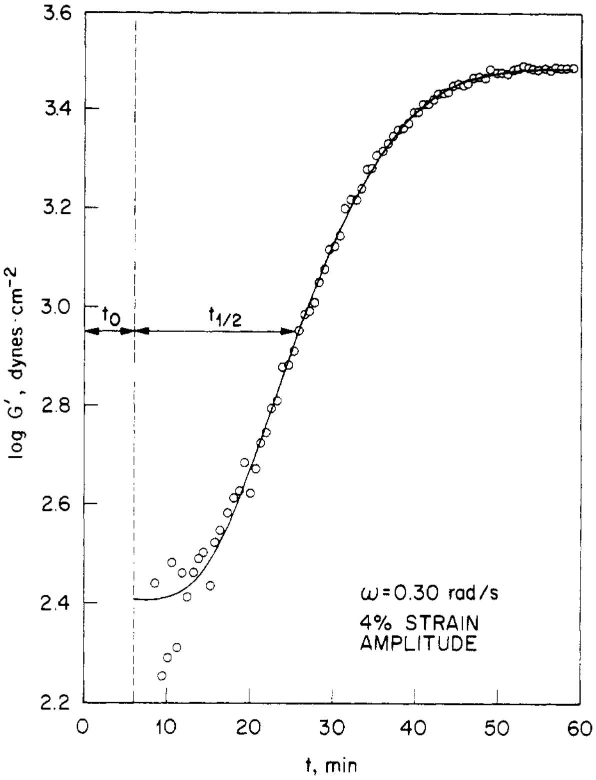

Figure 10. Evolution of G' in sample PEP-PEE-2 following a quench from the disordered state (T = 100 °C at t = 0) to 92 °C ($t = t_0$), which is 4° below T_{MST}. The solid curve is a fit to the Avrami equation. $t_{1/2}$ is defined as the time required to realize half the ultimate increase in log G'.

We presently make the assumption that $X(t)$ can be related to $G'(t)$ by

$$X(t) = \frac{G'(t) - G'_0}{G'_\infty - G'_0} \qquad (3)$$

where G'_0 and G'_∞ are the initial (just quenched) and asymptotic ($t \rightarrow \infty$) dynamic elastic moduli. An excellent fit of eqs 2 and 3 to the data can be obtained by adjusting n and t_0 (between 5 and 10 min due to the thermal equilibration time) as illustrated in Figure 10, where n varied from 2 to 4 depending on the quench temperature. While we cannot infer a microscopic mechanism from these results, they certainly suggest that a crystallization (i.e., ordering) process occurs for small amounts of supercooling.

Our primary use of the Avrami model has been to extract a characteristic ordering time $t_{1/2}$ defined here as the time required for half of the increase in log G' to occur following a temperature quench (see Figure 10). $t_{1/2}$ values are listed for seven quench temperatures in Table II where $1 \le \Delta T \le 7$ °C. For $\Delta T \gtrsim 7$ °C PEP-PEE-2 orders too rapidly for this measurement technique to be effective while the uncertainty in T (±1 °C) precludes rheometer-based kinetic experiments for $\Delta T \lesssim 1$ °C. In spite of these limitations the results in Table II show that a narrow window exists below the MST in which the ordering kinetics can be determined.

IV. Discussion

IV.A. Determining T_{MST}. The qualitative features of the dynamic shear moduli determined for PEP-PEE diblock copolymers in both the disordered and ordered states resemble those reported previously, particularly with respect to the 1,4-PB-1,2-PB diblock materials,[10] which are quite similar in composition, molecular weight,

Table II
Results from PEP-PEE-2 Temperature Quenches[a]

T,[b] °C	$t_{1/2}$,[c] min
95	976 ± 50
94	110 ± 13
93	25.7 ± 2.0
92	20.1 ± 3.0
91	9.5 ± 1.7
90	5.0 ± 0.5
89	3.7 ± 1.0

[a] Initial temperature prior to quench was 100 °C. [b] Subject to a systematic uncertainty of 1 °C. [c] $t_{1/2}$ is defined as the time required to attain half the ultimate increase in log $G'(t)$ following a temperature quench.

and entanglement density. In both PEP–PEE and 1,4-PB–1,2-PB the low-frequency regime in the ordered state, far from the MST, behaves as $G' \sim G'' \sim \omega^{0.5}$. This relation begins to break down as these materials are brought near the MST. At the MST G' and (less noticeably) G'' drop discontinuously as a consequence of disordering. Similar behavior has been observed in several studies involving SBS[2-4] and SIS[5] triblock copolymers. This discontinuity in rheological properties is a *natural consequence* of the *first-order nature of the MST.* In our judgement, isochronal ($\omega < \omega_c$) $G'(T)$ data obtained during heating (this avoids the hysteretic effects evident in the quenching experiments) represent the most precise and practical method for establishing T_{MST}.

Accurate determination of T_{MST} requires the acquisition of dynamic mechanical data well below a critical frequency, ω_c. We have established the critical frequencies for G' and G'' by making use of the time–temperature superposition principle. High-frequency ($\omega > \omega_c$) data are found to superimpose satisfactorily, producing the results illustrated in Figures 7 and 8. It is obvious from these plots that for log $(a_T\omega) \lesssim 0.5$ = log ω'_c and log $(a_T\omega) \lesssim -1.0$ = log ω''_c two branches appear in log $G'(a_T\omega)$ and log $G''(a_T\omega)$, respectively, as indicated by the filled and unfilled symbols. The gap between these two distinct branches occurs at T_{MST} (compare Figures 7 and 8 with Figure 1) and increases in size with decreasing reduced frequency. In order to observe a significant jump in G' and G'' at T_{MST}, experiments must be conducted well below ω'_c and ω''_c, respectively. While use of the superposition principle is not strictly correct for this rheologically complex material, its application in this context has no direct bearing on our determination of T_{MST}. Obviously, superpositioning the data is quite useful in guiding the selection of an appropriate low frequency for use in the isothermal temperature scans.

Recently, Han and Kim[6] have proposed an alternative method for interpreting dynamic mechanical data in order to establish T_{MST} in block copolymers. Their approach relies on the familiar Cole–Cole plot (here $G'(\omega)$ versus $G''(\omega)$), which eliminates the nonrigorous use of time–temperature superposition. Han and Kim interpret a departure from temperature independence in a log $G'(\omega)$ versus log $G''(\omega)$ representation as evidence of the microphase separation transition. In Figure 11 we have recast the results from Figures 7 and 8 in this modified Cole–Cole format. The qualitative features of this plot bear a striking resemblance to Figure 7, essentially validating our use of time–temperature superposition. However, the onset of a temperature dependence occurs between 146 and 135 °C, which is 39–50 °C above the actual MST. As discussed further below, this *continuous* departure from temperature-independent behavior begins when fluctuation effects become rheologically significant and should not be used as evidence for the MST.

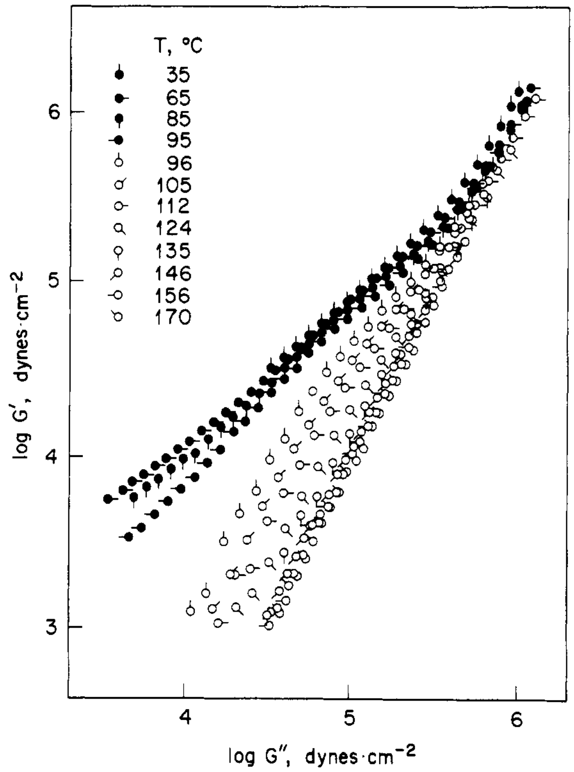

Figure 11. Modified Cole–Cole plot of the data presented in Figures 7 and 8.

Prior misinterpretation of this feature appears to derive from a lack of low-frequency ($\omega \ll \omega_c$) data combined with a large temperature increment (15 °C) between measurements on the SIS system.[6]

The location of the microphase separation transition is predicted to depend on the composition, f, the Flory–Huggins interaction parameter, χ, and the degree of polymerization, N.[11,12] For $f = 0.55$

$$(\chi N)_{\mathrm{MST}} = 10.7 + 43.16\bar{N}^{-1/3} \qquad (4)$$

with

$$\bar{N} = (a^6/v^2)N \qquad (5)$$

where a and v are the statistical segment length and volume, respectively. The constant term appearing in eq 4 corresponds to the mean-field prediction[11] while the term proportional to $\bar{N}^{-1/3}$ is a fluctuation correction.[12] In general, the segment–segment interaction parameter is linear with inverse temperature; i.e., $\chi = AT^{-1} + B$. The precise determination of T_{MST} for samples PEP-PEE-2 and PEP-PEE-3 along with our accurate measurements of N_w (Table I) allow us to estimate the coefficients A and B for $f = 0.55$. We base this calculation on an M_0 = 56 g/mol (i.e., a PEE) repeat unit. Assuming no excess volume of mixing with $\rho_{\mathrm{PEE}} = 0.870$ and $\rho_{\mathrm{PEP}} = 0.855$ g/cm^3 at 23 °C[21] gives $v = 1.079 \times 10^{-22}$ cm^3. A typical polymer melt thermal expansivity,[22] $v^{-1}\partial v/\partial T = 6.5 \times 10^{-4}$ K^{-1}, is also assumed. As described elsewhere[18] we have determined ln $a = -1.10 \times 10^{-3}T + 2.38$ Å for an f = 0.55 PEP–PEE diblock copolymer based on SANS measurements. With these parameters we obtain

$$\chi = 4.69/T + 4.44 \times 10^{-4} \qquad (6)$$

Unlike the 1,4-PB–1,2-PB system where the constant (i.e., entropy) term dominates χ,[23] here it represents only 6% of the interaction parameter midway between the two measurement temperatures.

IV.B. Fluctuation Effects. The limiting rheological characteristics in the disordered and ordered states are illustrated in Figures 5 and 6, respectively. In both cases the PEP–PEE results are virtually identical with the corresponding 1,4-PB–1,2-PB data described previously.[10] Well above the MST the block copolymer behaves like a homopolymer (see Figure 5), while far below the MST the dynamic mechanical response exhibits a nonterminal power law behavior (see Figure 6). This ordered-structure response bears a striking resemblance to that obtained from critical gels.[24] However, we are unable at this point to suggest a microscopic model, consistent with both a gel structure and a microphase-separated block copolymer, which recovers $G' \sim G'' \sim 0.5$. In fact, at present we cannot ascribe a detailed structure, e.g., polycrystalline versus random bicontinuous lamellae, to these ordered materials.

The rheological behavior of PEP–PEE-2 also closely resembles that of the corresponding 1,4-PB–1,2-PB sample[10] (i.e., BB6). Above approximately 146 °C this material responds like PEP–PEE-1. As the temperature is lowered, below 146 °C, a new relaxation mode becomes evident for $\omega < \omega_c$, which shifts to lower reduced frequencies with decreasing temperature. We can now definitively assign this response to transient concentration fluctuations based on SANS measurements obtained from a partially deuterated PEP–PEE sample near T_{MST}.[19] This conclusion is also consistent with dielectric spectroscopy data obtained from the nearly symmetric 1,4-PB–1,2-PB materials.[25]

At temperatures well above T_{MST} the amplitudes of the concentration fluctuations, which have a characteristic block copolymer period $D \approx 3R_g$ for $f = 0.55$,[11,12] are relatively small and accordingly exert little influence over the low-frequency properties. As the temperature approaches T_{MST}, the concentration fluctuation amplitude increases significantly, thereby impeding the long-range motion of individual block copolymer chains (recall that $\omega_c\tau_d \ll 1$). However, above the MST there is no permanent pattern established, and at sufficiently long times (low frequencies) the system still behaves as a liquid. This can be readily seen in Figure 7. Thus we can interpret the pronounced shoulder on the low-frequency $T \geq 96$ °C data in Figure 7 as deriving from a "pattern" relaxation mode. Just above the MST this "pattern mode" leads to more than a 1 order of magnitude increase in the dynamic elastic modulus over that which would characterize the nonfluctuating system; superposing the $T \geq 146$ °C data facilitates this comparison. A description of the disordered state morphology (i.e., pattern) derived from a combined rheological and SANS study of a partially deuterated PEP–PEE sample is presented in a separate report.[18]

In a series of papers, Fredrickson and co-workers have developed a theory for the low-frequency rheological properties of block copolymers near the MST. The most recent of these publications,[15] which incorporates fluctuation effects, is most relevant to the present work. Although a detailed analysis of their theory is beyond the scope of this discussion, Fredrickson and Helfand[15] provide two specific predictions, which can be evaluated using the results from PEP–PEE-2. For the symmetric case ($f = 1/2$) at the MST they predict

$$\left.\frac{\delta G'(\omega)}{G'_0(\omega)}\right|_{\omega\to0} = \frac{0.1N_e\bar{N}^{1/3}}{N} \qquad (7)$$

and

$$\left.\frac{\delta G''(\omega)}{G''_0(\omega)}\right|_{\omega\to0} = \frac{0.4N_e}{N} \qquad (8)$$

where $G'_0(\omega)$ and $G''_0(\omega)$ are the "bare" (i.e., fluctuation free) dynamic moduli, δ refers to the fluctuation contribution, $\omega \to 0$ specifies the terminal regime, and N_e is the entanglement degree of polymerization. Using $N_{e,\mathrm{PEP}} = 21$ and $N_{e,\mathrm{PEE}} = 191$[26] as upper and lower bounds on N_e, we calculate a 5–44% fluctuation contribution to G', which is more than 1 order of magnitude less than what is measured for PEP–PEE-2 at 96 °C (see Figure 7). However, the ratio of eqs 7 and 8 is 5.5, which accurately accounts for the asymmetric influence of fluctuation effects on G' and G''; comparison of Figures 7 and 8 shows approximately a 6-fold greater increase in G' relative to G'' due to fluctuations at 96 °C. These findings are in close agreement with those reported earlier for 1,4-PB–1,2-PB.[10]

Below T_{MST} a permanent pattern is established in a block copolymer. Here the low-frequency behavior changes qualitatively as previously described. Because this pattern is both permanent and (in principle) long-range, it is extremely sensitive to strain,[17] which accounts for the nonlinear behavior observed in Figure 1 below T_{MST}. A more quantitative treatment of this issue is also taken up elsewhere.[18]

In addition to nonlinear effects we have observed a considerable temperature dependence to G' and G'' in sample PEP–PEE-2 below the MST. This is not surprising since fluctuation effects are expected to be manifested on either side of the MST[18] analogous to what occurs around a critical point in binary mixtures. However, unlike the fluctuation effects above the MST, which produce essentially a linear viscoelastic response, those below the transition cannot be evaluated quantitatively. Nevertheless, sufficiently far below the MST, i.e., for samples PEP–PEE-3 (not shown) and PEP–PEE-4 (Figure 6), the influence of fluctuations clearly becomes insignificant.

Although we have not observed any discontinuity in the WLF parameters for sample PEP–PEE-2 at the MST (see inset in Figure 9), the effects of microphase separation do become apparent when all four diblock copolymers are considered together. As illustrated in Figure 9 there is a noticeable jump in the shift factor curves in going from PEP–PEE-1 to PEP–PEE-2, -3, and -4. This behavior is not surprising given our understanding of fluctuations.

Because the segregation of a block copolymer is restricted to molecular dimensions, unfavorable segment–segment interactions can only be relieved through the development of composition fluctuations. These increase in amplitude with decreasing temperature, i.e., with increasingly unfavorable mixing. As we have seen, such composition fluctuations can be manifested at a considerable distance from T_{MST}. As a consequence, sample PEP–PEE-2 is characterized by significant local segregation at all our measurement temperatures. Because these fluctuations relax at frequencies less than ω_c, the high-frequency data, which were used to extract the WLF parameters, reflect a segregated state. However, only a small jump in amplitude is predicted[12] at the MST; note it is the establishment of a permanent long-range pattern that leads to changes in the $\omega < \omega_c$ properties. Therefore, it is understandable that based on high-frequency measurements sample PEP–PEE-2 resembles PEP–PEE-3 and PEP–PEE-4 in Figure 9. In the case of PEP–PEE-1, which lies much further above the MST (we estimate $T_{\mathrm{MST}} = -72$ °C based on eqs 4–6), fluctuation effects are greatly diminished and accordingly this material behaves differently than the locally segregated samples.

We note that these arguments will not apply to binary liquid mixtures where the approach to a critical point leads to a divergent composition fluctuation correlation length, but the amplitude of the fluctuations remains small.

IV.C. Ordering Kinetics. The mean-field treatment of order and disorder in block copolymers by Leibler[11] predicts a stability limit just below the microphase separation transition, and a critical point for $f = 1/2$. On the basis of this theory, Hashimoto[27] recently proposed a time-dependent Ginzburg–Landau (TDGL) treatment for the ordering process in block copolymers following a temperature quench from the disordered state. This approach closely resembles traditional spinodal decomposition theory[28] with the free-energy function taken from Leibler's result. Thus, the instability is manifested at $q^* \sim R_g^{-1}$ rather than at $q = 0$ as occurs in unstable binary liquid mixtures.

Fredrickson and Helfand[12] have recently demonstrated that the introduction of fluctuation corrections to Leibler's theory completely suppresses the stability line ($T_s \rightarrow 0$ K), thus eliminating the second-order (i.e., continuous) critical point. Therefore, we do not expect Hashimoto's approach to correctly describe the ordering kinetics since, within the context of fluctuation theory, there is no stability limit. Instead, we anticipate a nucleation and growth mechanism, as is commonly encountered for systems undergoing a first-order transition.

Very recently Fredrickson and Binder[29] have developed a homogeneous nucleation and growth theory for nearly symmetric diblock copolymers based on the previously described fluctuation picture. These authors predict a narrow region of slow ordering kinetics just below the MST, consistent with our experimental findings (see Figure 10 and Table II). The predicted volume fraction of lamellar phase present at time t following a quench below T_{MST} can be closely approximated by the Avrami equation (eq 2) with $n = 4$. As illustrated in Figure 10, $G'(t)$ is well represented by the Avrami function although our estimates for n vary between approximately 2 and 4.

Based on our definition of $t_{1/2}$ (see section III.C) and with $f = 0.55$ and $\bar{N} = 1.1 \times 10^4$ ($T = 96$ °C), the Fredrickson–Binder theory reduces to

$$t_{1/2} \approx 0.02\tau_d\delta^{-3/4}\exp\left(\frac{\beta\Delta F^*}{4}\right) \tag{9}$$

with the free-energy barrier given by

$$\beta\Delta F^* = 0.23_5\bar{N}^{-1/3}\delta^{-2} \tag{10}$$

where τ_d is the terminal relaxation time, $\beta = (k_BT)^{-1}$, and

$$\delta = \frac{\chi - \chi_{\mathrm{MST}}}{\chi_{\mathrm{MST}}} \tag{11}$$

These equations represent a classical nucleation theory with the traditional ΔT^{-2} exponential dependence replaced by $\Delta\chi^{-2}$. Defining a kinetic limit of metastability as $\beta\Delta F^*/4 = 1$,[29] we calculate an experimentally (i.e., kinetically) accessible supercooling gap of $\Delta T_k \cong 19$ °C for sample PEP–PEE-2; note that ΔT_k is essentially dictated by the exponential term in eq 9. This predicted supercooling gap size is qualitatively consistent with our experimental findings (Table II).

Since the barrier term in eq 9 dominates the temperature dependence of $t_{1/2}$, a plot of ln $t_{1/2}$ versus δ^{-2} should yield a linear relationship. This is not found as illustrated in Figure 12a. Furthermore, the slope ($\sim\Delta F^*$) is everywhere at least 1 order of magnitude smaller than the prediction (solid line). Although these initial experiments are rather crude (yet reproducible), the difference between theory and experiment is sufficiently great that we believe homogeneous (i.e., primary) nucleation is not the controlling mechanism. This circumstance is well-known in homopolymer (e.g., polyethylene) crystallization where secondary nucleation determines the crystallization kinetics at moderate undercoolings.[30] By analogy with homopolymers, where the rate of crystallization is known to depend exponentially on ΔT^{-1} rather than ΔT^{-2}, we have also plotted our kinetic results in terms of δ^{-1} in Figure 12b. On the basis of $T_{\mathrm{MST}} = 96$ °C, the data again fail to linearize. Owing to the close proximity of our quench temperatures to the MST, the data reductions as illustrated in Figure 12 are extremely sensitive to the determination of T_{MST}. As we have stated, the temperature control over the rheometer leaves a 1 °C uncertainty in our determination of the transition temperature (see Figure 1). Therefore, we also show the δ^{-2} and δ^{-1} plots for $T_{\mathrm{MST}} = 97$ °C in Figure 12. This modification fails to linearize the homogeneous nucleation plot but does bring the secondary nucleation representation into a linear form. This result together with the gross overestimation of ΔF^* by the homogeneous nucleation theory leads us to tentatively conclude that heterogeneous (secondary) nucleation governs the ordering process near the MST. We will further explore this interesting aspect of block copolymer dynamics in future work.

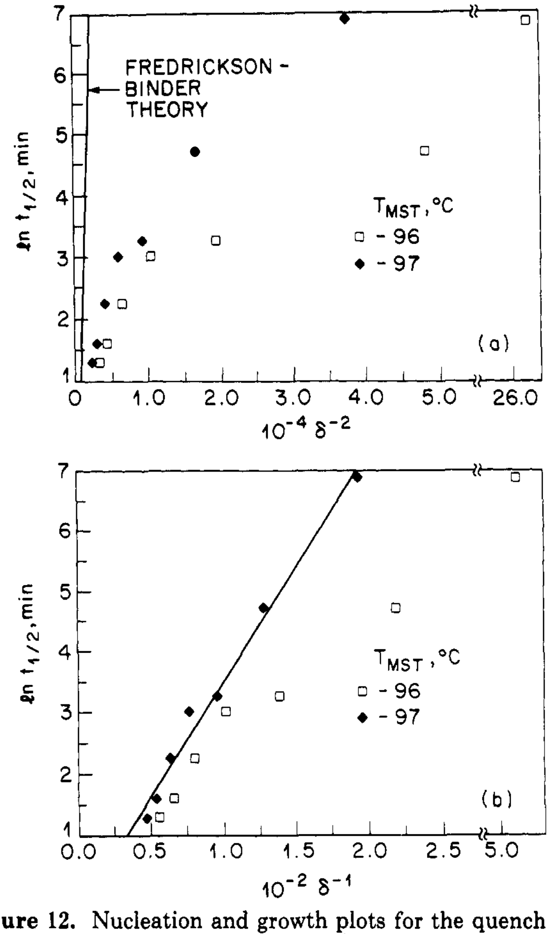

Figure 12. Nucleation and growth plots for the quench data from sample PEP–PEE-2 for two MST temperatures where $\delta = (\chi - \chi_{\mathrm{MST}})/\chi_{\mathrm{MST}}$: (a) homogeneous (primary) nucleation, (b) heterogeneous (secondary) nucleation. The linear form obtained with $T_{\mathrm{MST}} = 97$ °C in b indicates that heterogeneous nucleation is the controlling mechanism in the ordering process.

V. Summary and Conclusions

A rheological investigation of order and disorder in a nearly symmetric set of poly(ethylenepropylene)–poly(ethylethylene) (PEP–PEE) diblock copolymers has been presented. This study completely corroborates our earlier findings regarding 1,4-polybutadiene–1,2-polybutadiene diblock copolymers near the microphase separation transition (MST).[10] In particular, fluctuation effects have been shown to strongly influence the dynamic elastic and loss moduli below a critical reduced frequency, ω_c, both above and below the MST. These fluctuation effects are evident as much as 50° above the transition temperature. At the MST there exists a distinct discontinuity in G' and G'' for $\omega < \omega_c$, which provides a precise method for identifying the transition temperature.

Just below the MST lies a narrow range of temperatures ($T_{\mathrm{MST}} - T \lesssim 10$ °C) within which the ordering process (following a quench from the disordered state) is sufficiently slow so as to allow the quantitative evaluation of nucleation and growth kinetics. Initial experiments indicate that for such shallow quenches ordering occurs via a heterogeneous (secondary) nucleation process.

On the basis of the striking similarity between the presently reported results and those published earlier,[10] we conclude that these phenomena are universal for all symmetric diblock copolymers above the entanglement molecular weight. Future efforts in this area will examine how varying composition and chain architecture (e.g., triblock versus diblock) influences the low-frequency rheological properties near the order–disorder transition.

References and Notes

(1) Herman, D. S.; Kinning, D. J.; Thomas, E. L.; Fetters, L. J. *Macromolecules* **1987**, *20*, 2940.
(2) Chung, C. I.; Gale, J. C. *J. Polym. Sci., Polym. Phys. Ed.* **1976**, *14*, 1149.
(3) Gouinlock, E. V.; Porter, R. S. *Polym. Eng. Sci.* **1977**, *17*, 535.
(4) Chung, C. I.; Lin, M. I. *J. Polym. Sci., Polym. Phys. Ed.* **1978**, *16*, 545.
(5) Widmaier, J. M.; Meyer, G. C. *J. Polym. Sci., Polym. Phys. Ed.* **1980**, *18*, 2217.
(6) Han, C. D.; Kim, J. *J. Polym. Sci., Polym. Phys. Ed.* **1987**, *25*, 1741.
(7) Han, C. D.; Kim, J.; Kim, J. K. *Macromolecules* **1989**, *22*, 383.
(8) Cohen, R. E.; Ramos, A. R. *Macromolecules* **1979**, *12*, 131.
(9) Cohen, R. E.; Wilfong, D. E. *Macromolecules* **1982**, *15*, 370.
(10) Bates, F. S. *Macromolecules* **1984**, *17*, 2607.
(11) Leibler, L. *Macromolecules* **1980**, *13*, 1602.
(12) Fredrickson, G. H.; Helfand, E. *J. Chem. Phys.* **1987**, *87*, 697.
(13) Ferry, J. D. *Viscoelastic Properties of Polymers*, 3rd ed.; Wiley: New York, 1980.
(14) Bates, F. S.; Bair, H. E.; Hartney, M. A. *Macromolecules* **1984**, *17*, 1987.
(15) Fredrickson, G. H.; Helfand, E. *J. Chem. Phys.* **1988**, *89*, 5890. Fredrickson, G. H.; Larson, R. G. *J. Chem. Phys.* **1987**, *86*, 1553.
(16) Bates, F. S.; Rosedale, J. H.; Bair, H. E.; Russell, T. P. *Macromolecules* **1989**, *21*, 2557.
(17) Hadziioannou, G.; Mathis, A.; Skoulios, A. *Colloid Polym. Sci.* **1979**, *257*, 136.
(18) Bates, F. S.; Rosedale, J. H.; Fredrickson, G. H. *J. Chem. Phys.*, to appear.
(19) Bates, F. S.; Rosedale, J. H.; Fredrickson, G. H.; Glinka, C. J. *Phys. Rev. Lett* **1988**, *61*, 2229.
(20) Avrami, M. *J. Chem. Phys.* **1939**, *7*, 1103; **1940**, *8*, 212; **1940**, *9*, 177.
(21) ρ_{PEE} and ρ_{PEP} were determined using the density gradient column technique.
(22) Brandrup, J., Immergut, E. H., Eds. *Polymer Handbook*, 2nd ed.; Wiley: New York, 1975.
(23) Bates, F. S.; Hartney, M. A. *Macromolecules* **1985**, *18*, 2478.
(24) Hess, W.; Vilgas, T. A.; Winter, H. H. *Macromolecules* **1988**, *21*, 2536.
(25) Quan, X.; Johnson, G. E.; Anderson, E. W.; Bates, F. S. *Macromolecules* **1989**, *22*, 2457.
(26) Lin, Y. H. *Macromolecules* **1987**, *20*, 3080.
(27) Hashimoto, T. *Macromolecules* **1987**, *20*, 465.
(28) Cahn, J. W. *J. Chem. Phys.* **1965**, *42*, 93.
(29) Fredrickson, G. H.; Binder, K., submitted for publication in *J. Chem. Phys.*
(30) Bassett, D. C. *Principles of Polymer Morphology*; Cambridge Univeristy Press: Cambridge, England, 1981.